

Stress Intensity Factor Calculation for Designing with Fiber-Reinforced Composite Materials

G. R. Heppler,* S. Friskin,† and J. S. Hansen‡

University of Toronto, Toronto, Ontario, Canada

A singular finite element model of a cracked composite plate is employed to determine the variation of the mode I stress intensity factor for a center cracked plate with laminate configuration changes. Two material systems, T300/5208 and K49/934, are studied for seven crack length to specimen width ratios. A correlation between the basic material parameters and the stress intensity factors is presented which allows rapid, inexpensive estimation of the effect of laminate design changes given a bare minimum of initial data.

Nomenclature

A	= laminate stress resultant-strain constitutive relation
A'	= constitutive relation for an equivalent single ply laminate
C	= compliance matrix
e_{ij}	= tensor strain $i, j = 1, 2$
E_{11}, E_{22}	= lamina modulus in 1 and 2 directions
E_{xx}, E_{yy}	= laminate modulus in x and y directions
E'_{xx}, E'_{yy}	= equivalent lamina moduli
G_{12}, G'_{xy}, G'_{xy}	= corresponding shear moduli
h_k	= see Fig. 4
K_I, K_{II}, K_{est}	= stress intensity factors, mode I, mode II, and estimated
L	= crack semilength
Q, \bar{Q}	= lamina constitutive relations
N_i	= basis functions $i = 1, 12$
r, θ	= crack tip centered polar coordinates
s, t	= normalized conventional element coordinates
s_1, s_2	= roots of characteristic quartic
s	= a general value of $1/ s_1 s_2 $
t	= total laminate thickness
T	= transformation matrix
u, v	= membrane displacements
u_c, v_c	= conventional field component of u, v
u_s, v_s	= singular field component of u, v
v_1, v_{II}	= mode I displacement field contribution
u_{II}, v_{II}	= mode II displacement field contribution
W	= specimen semiwidth
ν_{12}, ν_{xy}	= Poisson's ratio
σ_{ij}	= stress components $i, j = 1, 2$
$\epsilon_{11}^0, \epsilon_{22}^0, \gamma_{12}^0$	= midplane strains (engineering)

Introduction

FIGER-REINFORCED composite materials are being incorporated in the design of an ever broadening range of structural components. This is because these materials have very attractive strength and stiffness-to-weight ratios and because of the design flexibility which they allow in the choice of mechanical, thermal, and vibrational characteristics. With

this flexibility, it is not surprising that composite materials are often employed in optimized designs, which raises valid concerns with regard to the understanding of the mechanisms as well as possibilities of failure.

If the fracture of these laminates is considered from the point of view of linear elastic fracture mechanics, the engineer must be concerned with two distinct aspects of a design: 1) the prediction of the stress intensity factor K_I , which depends on the applied stress in addition to the laminate configuration and specimen geometry, and 2) the experimentally determined values of the critical stress intensity factor K_c , which defines the onset of crack propagation as occurring when $K_I \geq K_c$. The present paper is concerned only with the first of these aspects, and deals with the calculation of K_I for a broad range of laminate configurations. These calculations represent an onerous if not time consuming and expensive task. Thus the aim in the present paper is to present the development of an economical and convenient method of estimating stress intensity factors that may be of use for the analysis and initial design phases of composite components. The integration of these results with critical stress intensity factors is discussed briefly in the conclusion of the paper.

A finite element analysis employing a high precision linear elastic fracture element¹ has been employed to determine the stress intensity factors associated with a prescribed laminate and a given crack length to specimen width ratio (L/W) for rectangular specimens subjected to uniaxial tension loading with a center crack. The crack-length-to-width ratios were varied from 0.2 to 0.8 and the tests were repeated for each of two unidirectional preimpregnated composite systems, T300/5208 and K49/934.

The results of this parameter study have been assembled into a concise and instructive representation that lends itself to use in design manual applications. An approximate method of interpolating between these data for different geometries and for material systems has also been developed to provide a convenient, inexpensive means of estimating the stress intensity factors for a wide variety of laminate designs.

It is assumed herein that these heterogeneous materials can be treated as homogeneous materials with regard to their macroscopic behavior. In this regard, indications from experiments are that when the zone of an elastic crack tip singularity contains a sufficient number of fibers, the homogeneous assumption is applicable.²

In the remainder of the paper the fracture element will be detailed, followed by a brief discussion of how the lamina material properties were utilized to provide the necessary data for the various laminates considered. Results from the application of the finite element method are presented, along with observations on some important correlations between K_I and L/W that are evident in the results. It will be illustrated

Received March 9, 1983; presented as Paper 83-0835 at the AIAA/ASME/ASCE/AHS 24th Structures, Structural Dynamics and Materials Conference, Lake Tahoe, Nev., May 2-4, 1983; revision received March 20, 1984. Copyright © American Institute of Aeronautics and Astronautics, Inc., 1983. All rights reserved.

*Research Engineer, Institute for Aerospace Studies. Member AIAA.

†Research Assistant, Institute for Aerospace Studies.

‡Associate Professor, Institute for Aerospace Studies.

how the lamina material parameters may be used to predict the stress intensity factor for a given L/W ratio provided K_I values are known for three prescribed laminates at that L/W ratio. The quality of the correlation between this empirical method and the finite element method is given, followed by overall conclusions.

Finite Element Formulation

A basic 12-node rectangular element^{1,3} is used for the conventional elements and also forms the basis for the enriched element formulation. The nodes for both types of elements are numbered as shown in Figs. 1 and 2. The corresponding basis functions are:

Corner nodes:

$$N_i = (1/32)(t+t_0)(1+s_0)[-10+9(t^2+s^2)] \quad (1)$$

Midside nodes:

$$t_i = \pm 1; \quad s_i = \pm \frac{1}{3}$$

$$N_i = (9/32)(1+t_0)(1-s^2)(1+9s_0)$$

The remaining midside node basis functions are obtained by interchanging t and s . Also, in the above, $t_0 = tt_i$ and $s_0 = ss_i$, where t_i and s_i are the values of t, s at the i th node, $s = x/a$ and $t = y/b$. Furthermore, it is understood that $N_i \equiv 0$ for $s, t \notin [-1, 1]$.

The displacement field associated with the crack tip is represented by⁴:

$$\begin{aligned} u_I &= K_I f_I(r, \theta), & v_I &= K_I g_I(r, \theta) \\ u_{II} &= K_{II} f_2(r, \theta), & v_{II} &= K_{II} g_2(r, \theta) \end{aligned} \quad (2)$$

where

$$\begin{aligned} f_I &= \sqrt{\frac{2r}{\pi}} \operatorname{Re} \left\{ \frac{1}{s_1 - s_2} [s_1 p_2 (\cos \theta + s_2 \sin \theta)^{1/2} \right. \\ &\quad \left. - s_2 p_1 (\cos \theta + s_1 \sin \theta)]^{1/2} \right\} \\ g_I &= \sqrt{\frac{2r}{\pi}} \operatorname{Re} \left\{ \frac{1}{s_1 - s_2} [s_1 q_2 (\cos \theta + s_2 \sin \theta)^{1/2} \right. \\ &\quad \left. - s_2 q_1 (\cos \theta + s_1 \sin \theta)]^{1/2} \right\} \\ f_2 &= \sqrt{\frac{2r}{\pi}} \operatorname{Re} \left\{ \frac{1}{s_1 - s_2} [p_2 (\cos \theta + s_2 \sin \theta)^{1/2} \right. \\ &\quad \left. - p_1 (\cos \theta + s_1 \sin \theta)]^{1/2} \right\} \\ g_2 &= \sqrt{\frac{2r}{\pi}} \operatorname{Re} \left\{ \frac{1}{s_1 - s_2} [q_2 (\cos \theta + s_2 \sin \theta)^{1/2} \right. \\ &\quad \left. - q_1 (\cos \theta + s_1 \sin \theta)]^{1/2} \right\} \end{aligned} \quad (3)$$

In the above, s_1 and s_2 are roots (in general complex) of

$$c_{11}s^4 - 2c_{16}s^3 + 2(c_{12} + c_{66})s^2 - 2c_{26}s + c_{22} = 0 \quad (4a)$$

where s_1, s_2 may be expressed as

$$s_1 = \alpha_1 + i\beta_1, \quad s_2 = \alpha_2 + i\beta_2 \quad (4b)$$

and the roots of interest are taken such that

$$\beta_1 > 0, \quad \beta_2 > 0$$

The additional coefficients in Eq. (3) are specified by

$$\begin{aligned} p_1 &= c_{11}s_1^2 + c_{12} - c_{16}s_1, & p_2 &= c_{11}s_2^2 + c_{12} - c_{16}s_2 \\ q_1 &= (c_{12}s_1^2 + c_{22} - c_{26}s_1)/s_1, & q_2 &= (c_{12}s_2^2 + c_{22} - c_{26}s_2)/s_2 \end{aligned} \quad (5)$$

In Eqs. (4) and (5), c_{ij} are the elements of the material compliance matrix C . Collecting the appropriate equations (2) yields the following:

$$u_s = u_I + u_{II}, \quad v_s = v_I + v_{II} \quad (6)$$

Finally, the displacement trial functions for the enriched element become,

$$u = u_c + u_s, \quad v = v_c + v_s \quad (7)$$

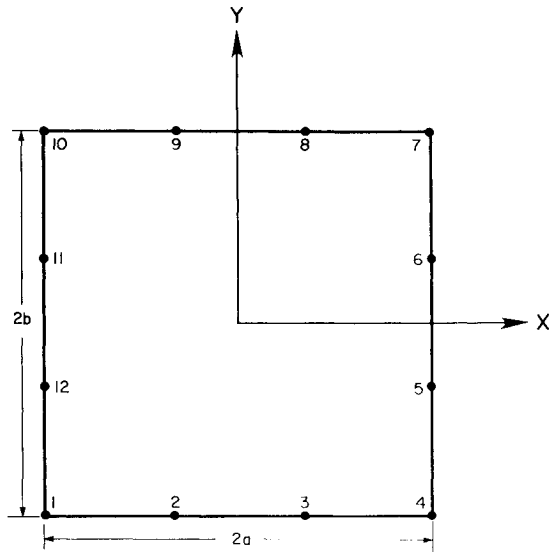


Fig. 1 Conventional element.

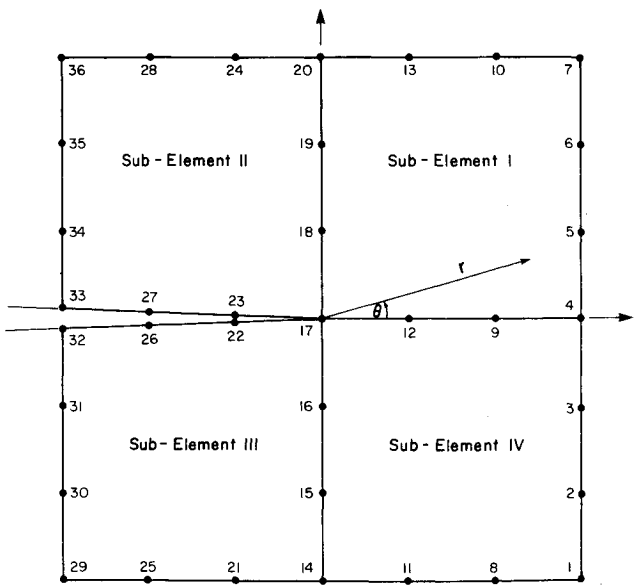


Fig. 2 Crack tip element.

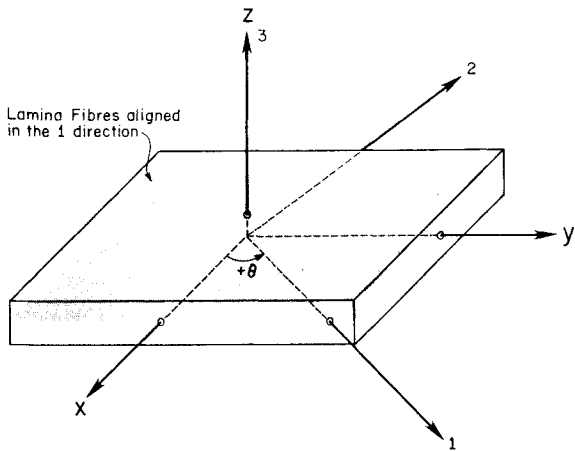


Fig. 3 Lamina-laminate coordinate frames.

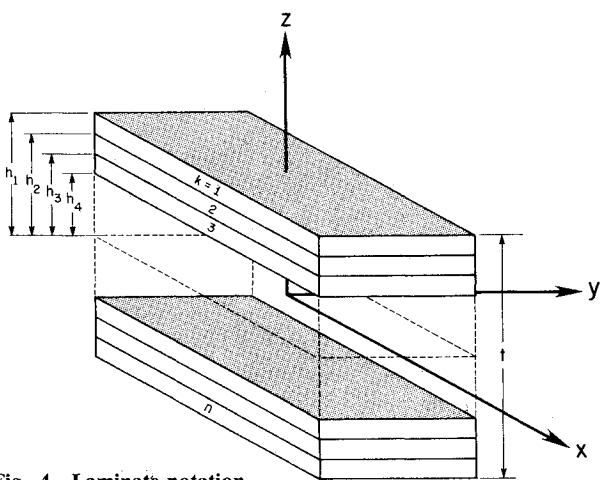


Fig. 4 Laminate notation.

Following Ref. 1 these are expressed as

$$\begin{aligned} u(s, t) &= \sum_{i=1}^{12} N_i u_i + \left[K_I \left(f_1 - \sum_{i=1}^{12} N_i f_{1i} \right) + K_{II} \left(f_2 - \sum_{i=1}^{12} N_i f_{2i} \right) \right] \\ v(s, t) &= \sum_{i=1}^{12} N_i v_i + \left[K_I \left(g_1 - \sum_{i=1}^{12} N_i g_{1i} \right) + K_{II} \left(g_2 - \sum_{i=1}^{12} N_i g_{2i} \right) \right] \end{aligned} \quad (8)$$

The finite element model that arises from this formulation has been shown¹ to be accurate to within 5% for $L/W \geq 0.3$. Larger errors are found to be associated with extreme element aspect ratios near $L/W = 0.2$.

Laminate Compliance Matrix

For a single orthotropic lamina in plane stress, the constitutive relation is given as

$$\begin{bmatrix} \sigma_{11} \\ \sigma_{22} \\ \sigma_{12} \end{bmatrix} = \begin{bmatrix} Q_{11} & Q_{12} & 0 \\ Q_{12} & Q_{22} & 0 \\ 0 & 0 & 2Q_{66} \end{bmatrix} \begin{bmatrix} e_{11} \\ e_{22} \\ e_{12} \end{bmatrix} \quad (9)$$

where the components of the Q_{ij} are:

$$Q_{11} = \frac{E_{11}}{(1 - \nu_{12}\nu_{21})} \quad (10a)$$

$$Q_{22} = \frac{E_{22}}{(1 - \nu_{12}\nu_{21})} \quad (10b)$$

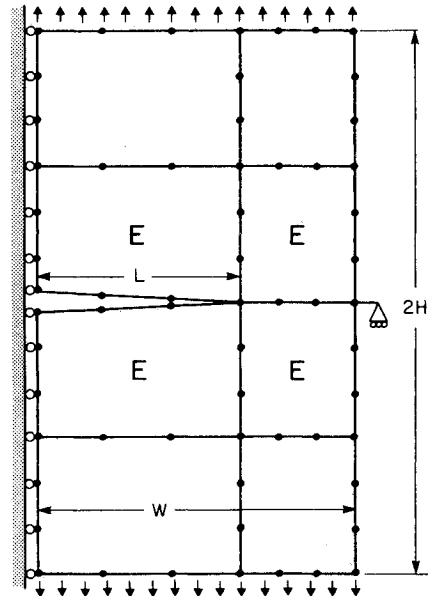


Fig. 5 Finite element model, enriched elements are marked "E".

Table 1 Lamina material properties

Material	T300/5208	K49/934
E_{11} , psi	20.5×10^6	11.0×10^6
E_{22} , psi	1.37×10^6	0.80×10^6
G_{12} , psi	0.752×10^6	0.3×10^6
ν_{12}	0.31	0.34

$$Q_{12} = \frac{\nu_{21}E_{11}}{(1 - \nu_{12}\nu_{21})} = \frac{\nu_{12}E_{22}}{(1 - \nu_{12}\nu_{21})} \quad (10c)$$

$$Q_{66} = G_{12} \quad (10d)$$

$$Q_{16} = Q_{26} = 0 \quad (10e)$$

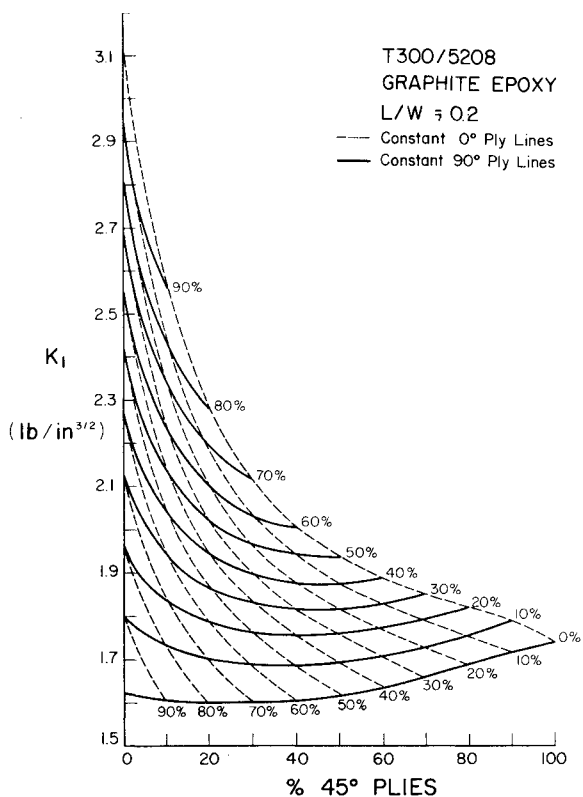
and where it is noted that tensor strains are to be employed. Now if the 1-2 axes of the lamina (Fig. 3) do not coincide with the geometric axes (x-y) of interest, relation (9) can be transformed to the new axis via

$$\begin{bmatrix} \sigma_{xx} \\ \sigma_{yy} \\ \sigma_{xy} \end{bmatrix} = T^{-1} QT \begin{bmatrix} e_{xx} \\ e_{yy} \\ e_{xy} \end{bmatrix} \quad (11)$$

where the transformation matrix is the usual second-order tensor transformation for rotation in a plane. Specifically

$$T = \begin{bmatrix} \cos^2\theta & \sin^2\theta & 2\sin\theta\cos\theta \\ \sin^2\theta & \cos^2\theta & -2\sin\theta\cos\theta \\ -\sin\theta\cos\theta & \cos\theta\sin\theta & \cos^2\theta - \sin^2\theta \end{bmatrix} \quad (12)$$

The product $T^{-1}QT$ is made symmetric by adopting engineering strains on the right-hand side of Eq. (11). The result of this adjustment is referred to as \bar{Q} . It is readily shown⁵ that for a laminate composed of n plies the matrix relating the stress resultants (N_x, N_y, N_{xy}) to the midplane strains ($\epsilon_{xx}^0, \epsilon_{yy}^0, \gamma_{xy}^0$)

Fig. 6 K_I for T300/5208 laminates, $L/W = 0.2$.

such that

$$\begin{bmatrix} N_x \\ N_y \\ N_{xy} \end{bmatrix} = A \begin{bmatrix} \epsilon_{xx}^0 \\ \epsilon_{yy}^0 \\ \gamma_{xy}^0 \end{bmatrix} \quad (13)$$

is given by (see Fig. 4)

$$A_{ij} = \sum_{k=1}^n (\bar{Q}_{ij})(h_k - h_{k-1}) \quad (14)$$

Laminates are restricted to symmetric balanced configurations in the present so that there will be no membrane-bending coupling and the resulting laminate will be orthotropic with respect to the geometric axes. This restriction is placed for computational convenience and there is, in principle, no reason why unbalanced configurations could not be treated in a manner similar to that presented here.

Since the laminate is being considered a homogeneous orthotropic material, A_{ij} can be equated to an A'_{ij} , which is derived from a single lamina of thickness t equal to the total laminate thickness and whose material axes coincide with the geometric axes. Thus for this single ply laminate

$$A_{ij} = A'_{ij} = Q'_{ij}t \quad (15)$$

A unit laminate thickness is assumed for all the following work; hence

$$A_{ij} = A'_{ij} = Q'_{ij} \quad (16)$$

This allows determination of the $E'_{xx}, E'_{yy}, G'_{xy}, \nu'_{xy}$, which will make the single-ply homogeneous orthotropic plate appear to be equivalent to the multi-ply laminated plate in a planar loading situation,

$$E'_{xx} = A_{11} - (A'_{12}/A_{22}) \quad (17a)$$

$$E'_{yy} = A_{22} - (A'_{12}/A_{11}) \quad (17b)$$

$$G'_{xy} = A_{66} \quad (17c)$$

$$\nu'_{xy} = (A_{12}/A_{22}) \quad (17d)$$

It is these equivalent material constants that are used to describe the mechanical characteristics of the plate which is to be analyzed.

The compliance matrix of the equivalent plate is given according to

$$\begin{bmatrix} e_{xx} \\ e_{yy} \\ e_{xy} \end{bmatrix} = \begin{bmatrix} \frac{1}{E'_{xx}} & \frac{-\nu_{21}}{E'_{yy}} & 0 \\ \frac{-\nu_{21}}{E'_{yy}} & \frac{1}{E'_{yy}} & 0 \\ 0 & 0 & \frac{1}{2G'_{xy}} \end{bmatrix} \begin{bmatrix} \sigma_{xx} \\ \sigma_{yy} \\ \sigma_{xy} \end{bmatrix} \quad (18)$$

Therefore

$$c_{11} = 1/E'_{xx} \quad (19a)$$

$$c_{12} = -\nu_{21}/E'_{yy} = -\nu_{12}/E'_{xx} = c_{21} \quad (19b)$$

$$c_{22} = 1/E'_{yy} \quad (19c)$$

$$c_{66} = 1/2G'_{xy} \quad (19d)$$

$$c_{16} = c_{26} = 0 \quad (19e)$$

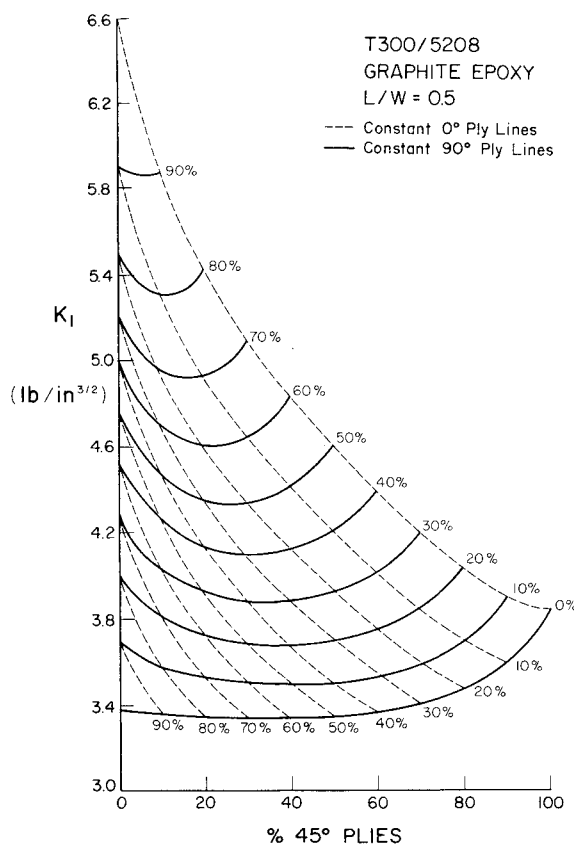
Laminates composed of varying proportions of 0° , $\pm 45^\circ$, and 90° plies have been chosen for illustration purposes since at least one major commercial airplane manufacturer has tried to design its composite components almost entirely of $(0^\circ, \pm 45^\circ, 90^\circ)$ combinations of woven lamina. The material systems chosen were T300/5208, a unidirectional graphite-epoxy system, and K49/934, a unidirectional Kevlar-49-epoxy system. The lamina material properties for these systems are given in Table 1.

Note that for the purpose of proportioning, all the plies with an absolute orientation of 45° are considered to be the same.

Finite Element Tests and Results

In the modeling of the cracked specimens, advantage was taken of the vertical line of symmetry and only one half of a specimen was analyzed. The model was taken to have a width W of 5 in. and a total height $2H$ of 10 in. and was divided into six elements, four equally proportioned elements in the vertical direction and two elements, of generally different widths, in the horizontal direction (Fig. 5). A unit tensile stress was applied.

Examples of the results obtained are illustrated for the T300/5208 material in Figs. 6-8, where the variation of mode I stress intensity factor with lamina configuration is shown for L/W ratios of 0.2, 0.5, and 0.8, respectively. These figures illustrate the variation of the K_I envelope as a function of L/W . Note that they are not drawn to the same scale. The variation in envelope geometry as a function of L/W is more clearly seen in Fig. 9, where the outlines of the envelopes for L/W ratios ranging between 0.2 and 0.8 are shown concurrently. The concise economy and versatility of a plot such as this can be immediately appreciated since it allows the designer to assess the effect of increasing or decreasing relative proportions of the various component ply angles without resorting to more time-consuming methods.

Fig. 7 K_I for T300/5208 laminates, $L/W = 0.5$.

Generally the shape of the envelope obtained is similar for all L/W ratios, with the spread of K_I values occurring in a specific envelope increasing proportionally to the L/W ratio.

It is usually the case that the K_I value for a laminate composed solely of 0° plies is the lowest value attained (an exception to this observation occurs where $L/W = 0.2$, Fig. 6) while the value associated with the 100% 90° laminate is the largest value reached. The 100% $\pm 45^\circ$ laminate takes on a value between these two extremes generally closer to the 0° value than the 90° value.

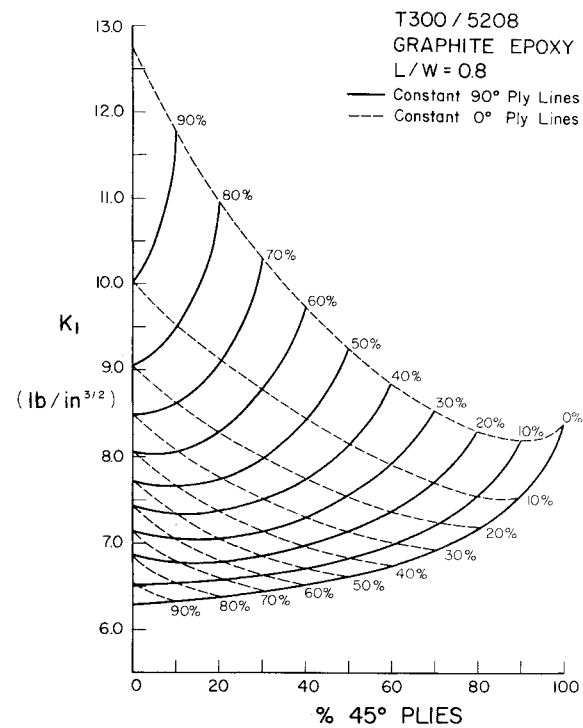
The gradients of the lines in the envelope increase quite rapidly as the proportions of $\pm 45^\circ$ and 0° plies are reduced, giving way to greater percentages of 90° plies. Thus for laminates composed primarily of 90° plies a slight adjustment in the laminate configuration can precipitate quite large changes in the value of the stress intensity factor.

Alternatively, for laminates composed primarily of 0° and $\pm 45^\circ$ plies slight changes in the lamina proportions will result in small changes in the value of the stress intensity factor. The more $\pm 45^\circ$ plies present, the less likely a manufacturing error will yield a significantly larger K_I value. For example, the effect of increasing the number of $\pm 45^\circ$ plies while keeping the number of 0° plies constant, or even close to constant, is seen to be a lowering of the value for K_I and a stabilization of K_I for additional changes in the number of 0° or 90° plies used.

Interpolation between L/W values is possible by noting that for the three 100% points $\log_{10} K_I$ varies in an approximately linear fashion with L/W (Fig. 10). The linearity breaks down slightly in the range of $L/W = 0.2$, which may be due to the larger errors expected from the finite element model in this range.¹

All the foregoing for the T300/5208 material system was found to hold true for the K49/934 system as well (Figs. 11-13).

During the course of this parameter study an interesting correlation between the material properties and the stress intensity factors was observed. Recall the previously introduced

Fig. 8 K_I for T300/5208 laminates, $L/W = 0.8$.

laminate parameters s_1 and s_2 [Eq. (4)]. It was found that when the reciprocal of the product of the absolute values of these parameters ($1/|s_1| |s_2|$) was plotted in a similar manner to the stress intensity values a figure of strikingly similar shape to the K_I envelopes was obtained (Figs. 14-15). This geometric similarity can be utilized to the designer's benefit. If the K_I values for some particular L/W ratio are known for laminates composed of all 0° , $\pm 45^\circ$, or 90° plies, respectively, which may be obtained either experimentally or numerically, then the complete envelope of stress intensity factors can be obtained approximately. This is accomplished by transforming the $1/|s_1| |s_2|$ plot to a K_I plot by utilizing the three known K_I values and an empirical transformation developed for this purpose.

Before outlining the development of the empirical transformation which takes the $1/|s_1| |s_2|$ envelope to a K_I envelope, some simplifying notation will be introduced. During this development the letters s and K will refer to a general value of $1/|s_1| |s_2|$ or K_I , respectively, and subscripts 0, 45, or 90 will refer to the value of either s or K associated with the laminate composed of 100% 0° , $\pm 45^\circ$, or 90° plies, respectively. For example K_0 is the value of K_I for a laminate made up of only 0° plies and s_{45} is the value of $1/|s_1| |s_2|$ for a laminate of all $\pm 45^\circ$ plies. A double subscript designates the curve joining the two subscript points.

Similarly, when reference is made to a 0° , 45° , or 90° point it is referring to the point on the envelope corresponding to 100% 0° , $\pm 45^\circ$, or 90° ply configuration.

The variable x will represent the horizontal degree of freedom on the envelope plots, specifically the fraction of $\pm 45^\circ$ plies present in the laminate, and it varies between zero and one.

If the K and s envelopes for a given L/W ratio and material system are plotted together, they would appear generally as illustrated in Fig. 16. It is assumed that the separation between each corresponding pair of the $s_{0,45}$ and $K_{0,45}$ curves and the $s_{90,45}$ and $K_{90,45}$ curves varies linearly with x . Thus, by knowing K_0 , K_{45} , K_{90} , and $s(x)$ on $s_{0,45}$ it follows that $K(x)$ on either $K_{0,45}$ or $K_{90,45}$ may be estimated from

$$K_{0,45}(x) = [K_{45} - s_{45} - K_0 + s_0]x + K_0 - s_0 + s_{0,45}(x) \quad (20a)$$

$$K_{90,45}(x) = [K_{45} - s_{45} - K_{90} + s_{90}]x + K_{90} - s_{90} + s_{90,45}(x) \quad (20b)$$

To find the shape of the interior of the envelope it is necessary to estimate the position of each of the interaction points on each vertical line corresponding to a constant proportion of $\pm 45^\circ$ plies ($x = \text{const}$).

A transformation has been found that accomplishes this. The complete estimated envelope of K_I values can be obtained from

$$K_{\text{est}} = \frac{[1 + \log_{10} s_x]^\alpha - [1 + \log_{10} s_{90,45}(x)]^\alpha}{[1 + \log_{10} s_{90,45}(x)]^\alpha - [1 + \log_{10} s_{0,45}(x)]^\alpha} \times [K_{90,45}(x) - K_{0,45}(x)] + K_{90,45}(x)$$

where

$$\alpha = \exp[2.935(L/W)^2 - 0.8655(L/W) + 0.0557]$$

and s_x is any value of $1/|s_1| |s_2|$ at a constant value of x .

The results of applying this mapping to the s plots for both the graphite and Kevlar material systems can be seen in Figs. 17-20 where the dashed lines of the inset figure correspond to the finite element results.

From these figures it is evident that the transformation maintains the same general shape and trends exhibited in the finite element results. Although there is some local divergence between the two envelopes the disagreement is sufficiently small, in light of the faithful reproduction of trends, to be of small concern when it is further acknowledged that the estimating procedure is intended to be just that—an estimate.

The disagreement between the finite element results and the estimated results varies with L/W ratio and material. For the T300/5208 material the maximum disagreement ranges from

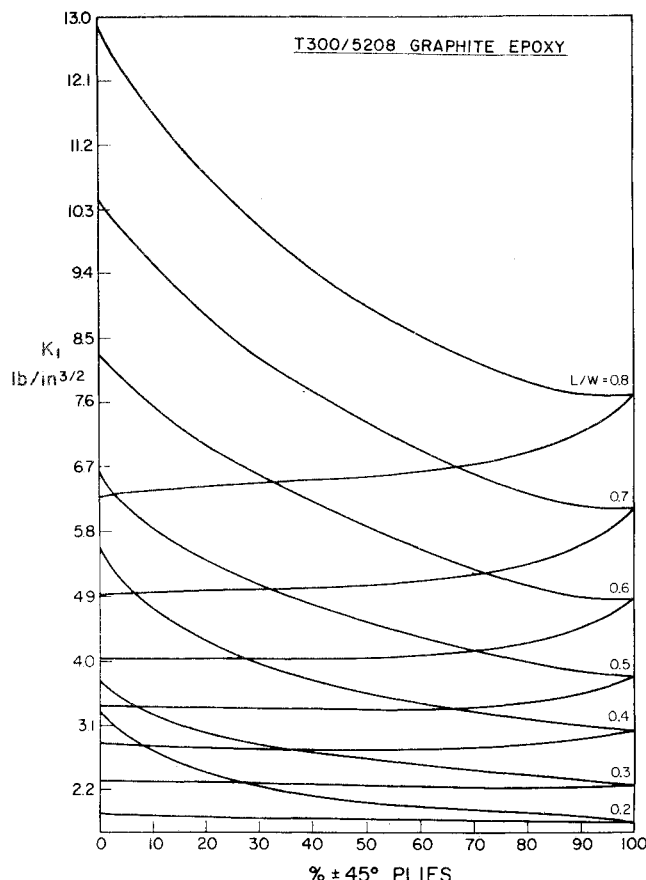


Fig. 9 K_I for T300/5208 laminates, envelope outlines.

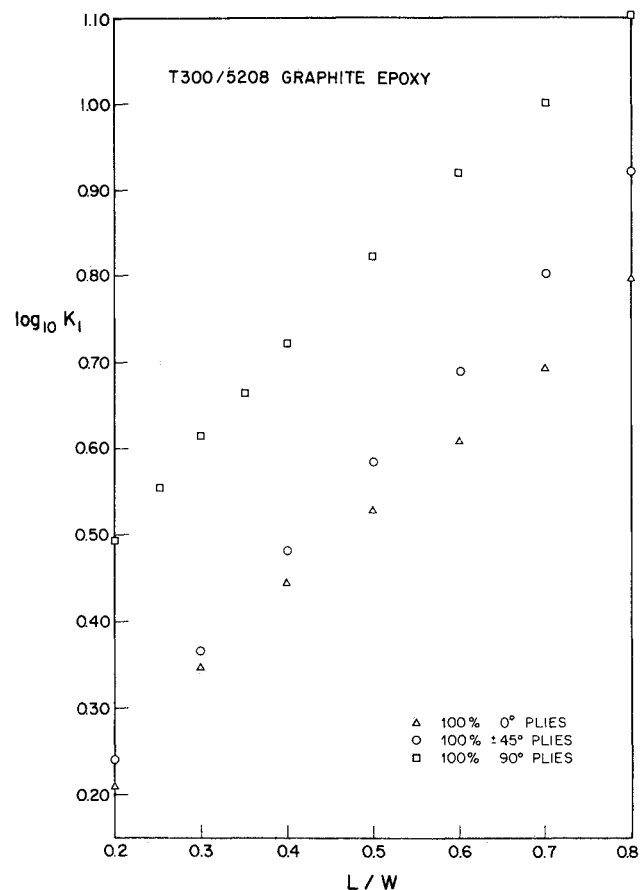


Fig. 10 $\log_{10} K_I$ vs L/W for T300/5208 (K_0, K_{45}, K_{90}).

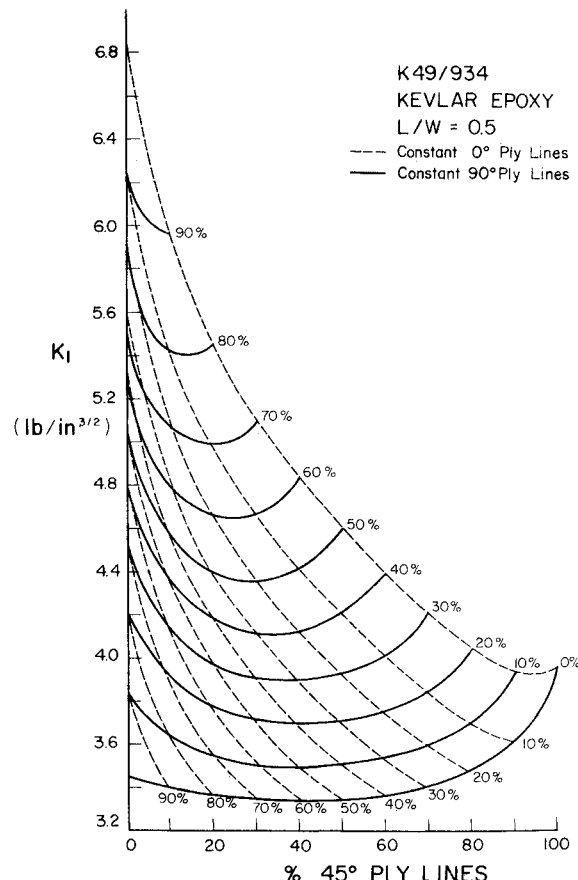
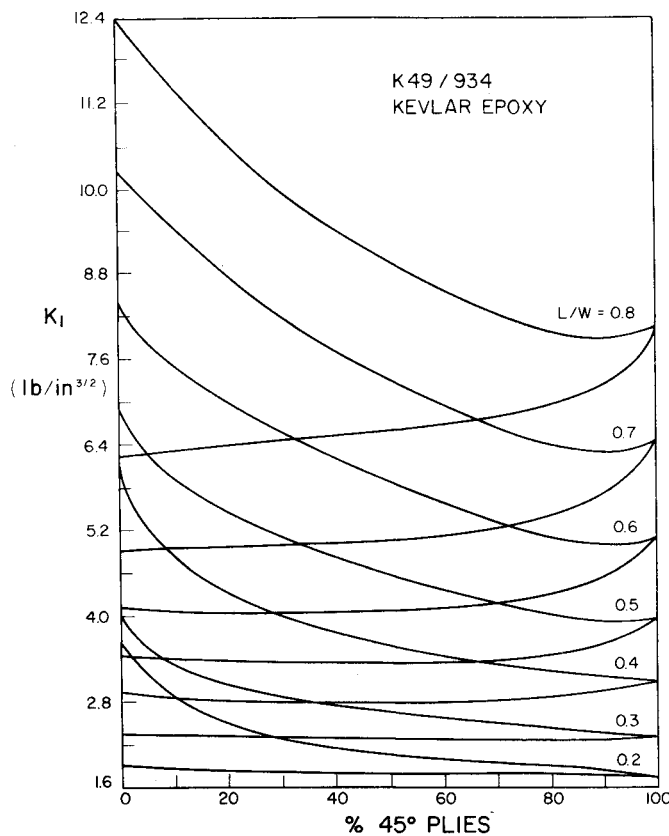
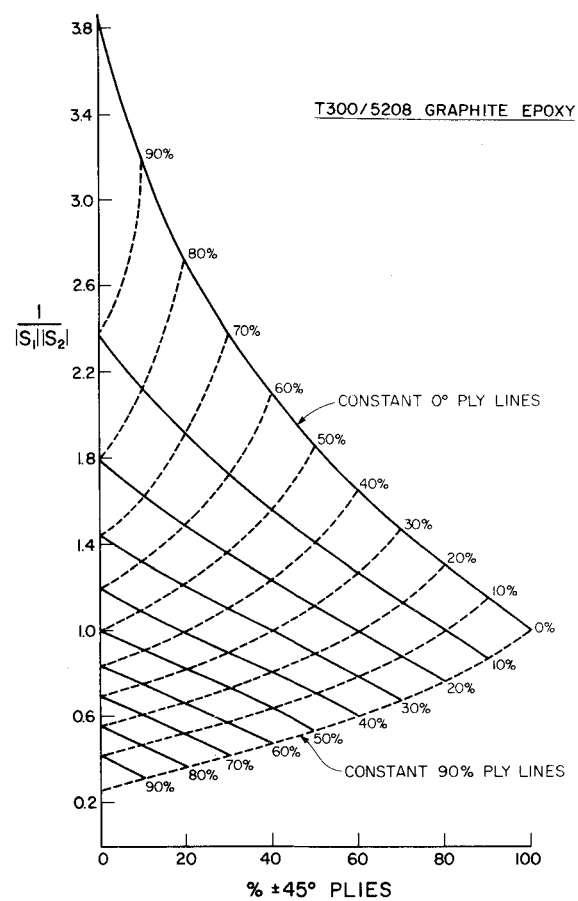
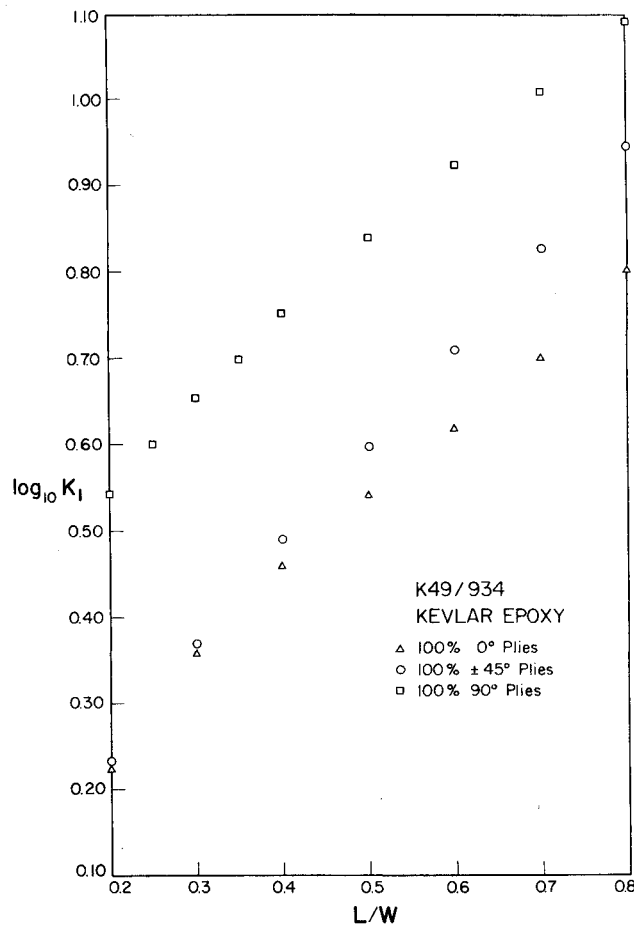
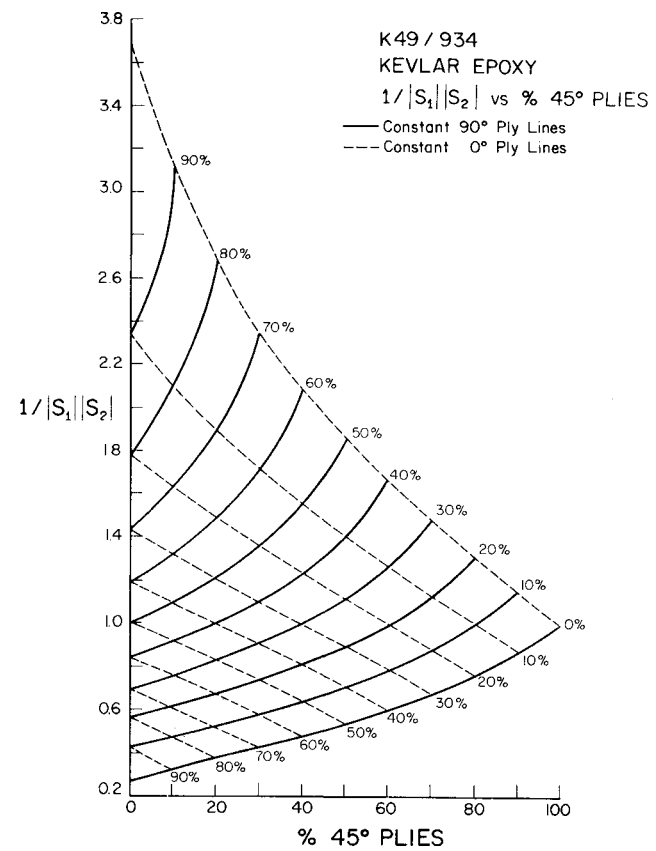
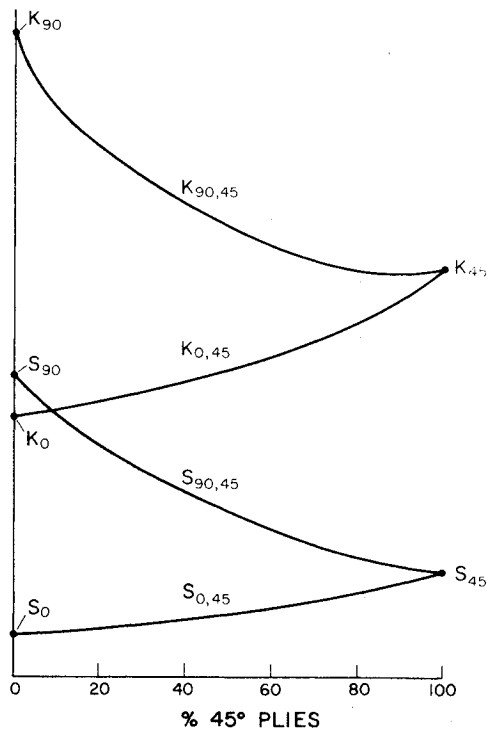
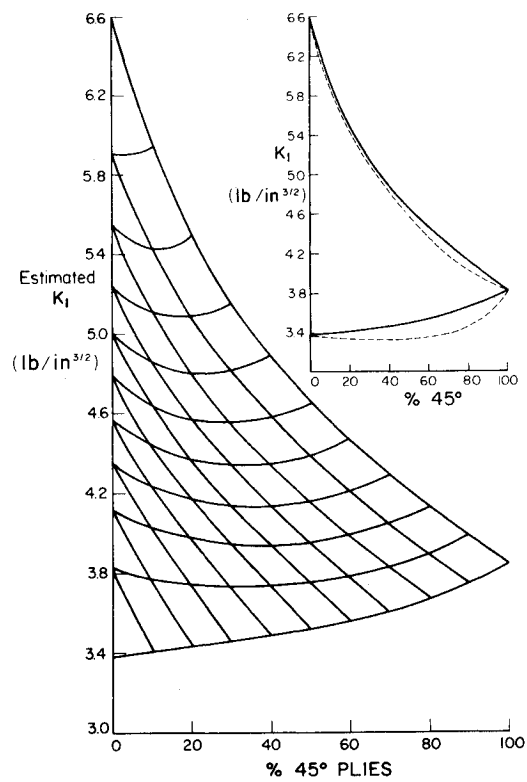
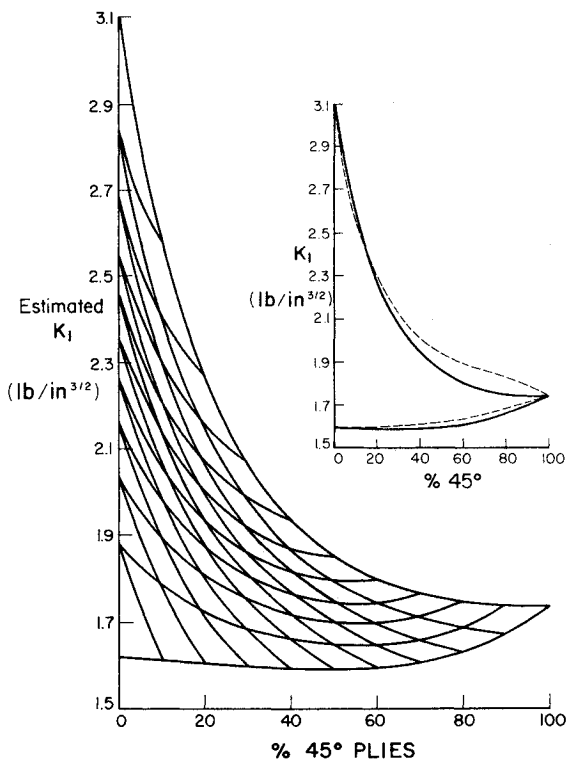
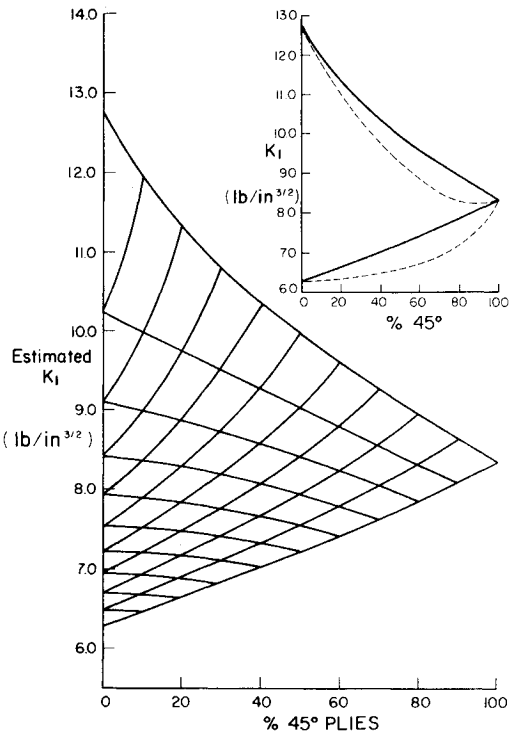


Fig. 11 K_I for K49/934 laminates, $L/W = 0.5$.

Fig. 12 K_I for K49/934 laminates, envelope outlines.Fig. 14 $1/|S_1||S_2|$ for T300/5208 laminates.Fig. 13 $\log_{10} K_I$ vs L/W for K49/934 (K_0, K_{45}, K_{90}).Fig. 15 $1/|S_1||S_2|$ for K49/934 laminates.

Fig. 16 Representative K and s plots.Fig. 18 K_{est} for T300/5208 laminates, $L/W=0.5$.Fig. 17 K_{est} for T300/5208 laminates, $L/W=0.2$.Fig. 19 K_{est} for T300/5208 laminates, $L/W=0.8$.

less than 5% for L/W ratios of 0.2-0.4 to 7%, 10%, 13%, and 12% for L/W ratios of 0.5, 0.6, 0.7, and 0.8, respectively. In the case of K49/934 the maximum disagreement encountered was 14% for $L/W=0.2$, 0.3, 0.6; 11% for $L/W=0.4$, 0.5; 16% for $L/W=0.7$; and 15% for $L/W=0.8$. Thus the maximum difference at any single point between the estimated stress intensity factors and the finite element stress intensity factors is 16%. As a quick means of estimating K_I values in initial or preliminary design stages, this method is very inexpensive in terms of computational effort and the degree of user

sophistication required to initiate an estimate. The method is easily programmed onto a desktop computer and allows immediate assessment of laminate design changes with regard to relative crack severity.

The material dependency of the accuracy of the estimating procedure is a matter of interest, and it may well be possible to derive another transformation that exhibits even greater accuracy. However, this will require further studies encompassing more material systems.

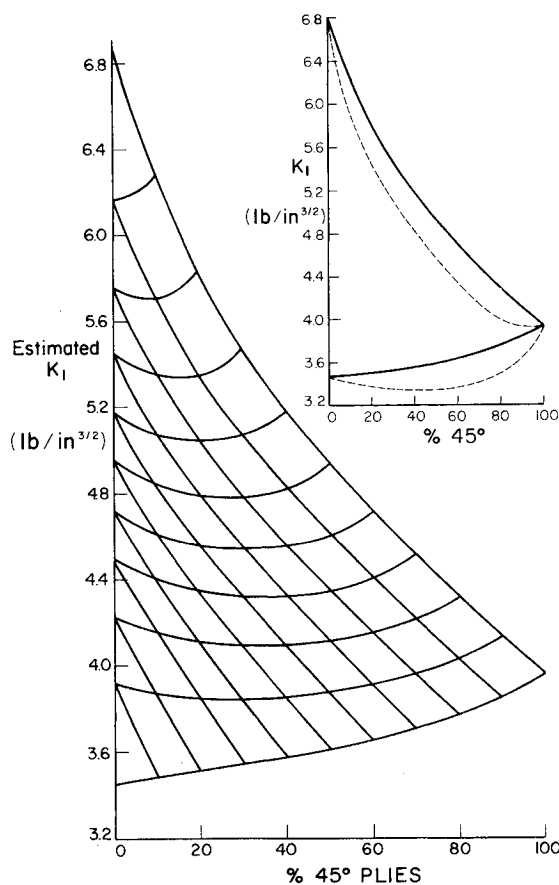


Fig. 20 K_{est} for K49/934 laminates, $L/W = 0.5$.

Summary

The investigation of how laminate configuration influences the value of K_1 illustrates that the general shape of the stress intensity factor envelopes does not change with material or L/W ratio apart from some dilation in the latter case. The sen-

sitivity of the stress intensity factor to laminate configuration changes depends on the relative proportion of each of the ply types ($0^\circ, \pm 45^\circ, 90^\circ$) with the sensitivity being reduced upon the addition of more $\pm 45^\circ$ plies. Large proportions of 90° plies make K_1 very sensitive to even slight changes in the laminate configuration.

A strong geometric similarity between the K_1 and $1/|s_1| |s_2|$ plots has been identified and means of utilizing this geometric similarity for estimating purposes shows promise. By knowing K_0 , K_{45} , and K_{90} for a particular material system and the L/W ratio, it is possible to estimate the entire K_1 envelope from the $1/|s_1| |s_2|$ envelope by utilizing the proposed transformation. The agreement between the finite element results and the estimated results is seen to be dependent on the L/W ratio and on the material system while it is sufficiently accurate for initial estimating purposes. It is felt that further correlation studies and transformation refinements may improve this approach.

It is important to realize that these results make no direct predictions about failure and that, as mentioned previously, companion data for the critical stress intensity factor K_c are required in order to decide the question of crack propagation. It may well be the case that K_c varies just as dramatically as K_1 over the same range of laminate configurations but this cannot be determined without a comprehensive set of experimental K_c data. If these data were available the designer would certainly prefer plots of the type presented here where the ordinate was the ratio K_1/K_c for example.

References

¹Heppeler, G. and Hansen, J. S., "Mixed Mode Fracture Analysis of Rectilinear Anisotropic Plates by High Order Finite Elements," *International Journal for Numerical Methods in Engineering*, Vol. 17, 1981, pp. 445-464.

²Snyder, M. D. and Cruse, T. A., "Crack Tip Stress Intensity Factors in Finite Anisotropic Plates," Air Force Materials Laboratory, AFML-TR-73-209, Aug. 1973.

³Zienkiewicz, O. C., *The Finite Element Method in Engineering Science*, 2nd Ed., McGraw-Hill, London, 1971, pp. 107-109.

⁴Sih, G. C. and Liebowitz, H., "Mathematical Theories of Brittle Fracture," *Fracture, an Advanced Treatise*, Vol. II, edited by H. Liebowitz, Academic Press, New York, 1968, pp. 108-131.

⁵Ashton, J. E., Halpin, J. C., and Petit, P. H., *Primer on Composite Materials*, Technomic Publishing, Westport, Conn., 1969.